Effect on the longitudinal coherence properties of pseudo thermal light source as a function of source size and temporal coherence

AZEEM AHMAD[1,2,3], TANMOY MAHANTY[1], VISHESH DUBEY[1,2], ANKIT BUTOLA[1], BALPREET SINGH AHLUWALIA[2], DALIP SINGH MEHTA[1,4]

[1]*Department of Physics, Indian Institute of Technology Delhi, Hauz Khas, New Delhi 110016, India*
[2]*Department of Physics and Technology, UiT The Arctic University of Norway, Tromsø 9037, Norway*
**Corresponding author: [3]ahmadazeem870@gmail.com, [4]mehtads@physics.iitd.ac.in*

Abstract: In the present letter, a synthesized pseudo thermal light source having high temporal coherence (TC) and low spatial coherence (SC) properties is used. The longitudinal coherence (LC) properties of the spatially extended monochromatic light source are systematically studied. The pseudo thermal light source is generated from two different monochromatic laser sources: He-Ne (@ 632 nm) and DPSS (@ 532 nm). It was found that the LC length of such light source becomes independent of the parent laser's TC length for large source size. For the chosen lasers, the LC length become constant to about 30 µm for laser source size of ≥ 3.3 mm. Thus, by appropriately choosing the source size, any monochromatic laser light source depending on the biological window can be utilized to obtain high axial-resolution in optical coherence tomography (OCT) system irrespective of its TC length. The axial resolution of 650 nm was obtained using 1.2 numerical aperture objective lens at 632 nm wavelength. These findings pave the path for widespread penetration of pseudo-thermal light into existing OCT systems with enhanced performance. Pseudo-thermal light source with high TC and low SC properties could be an attractive alternative light source for achieving high axial-resolution without needing dispersion-compensation as compared to the broadband light source.

Keywords: Coherence and statistical optics, Microscopy, Optical coherence tomography, Partial coherence in imaging.

Introduction: Coherence properties of light sources play a crucial role in various optical techniques such as profilometry, digital holographic microscopy, quantitative phase microscopy (QPM) coherence scanning profilometry and optical coherence tomography (OCT) [1-5]. Coherence is broadly classified into two categories: temporal and spatial coherence [6-8]. The spatial coherence (SC) is further divided into two sub-categories: lateral and longitudinal spatial coherence (LSC). The coherence gating generated due to the low temporal coherence (TC) length of broadband light sources have been widely utilized in Full-Field OCT (FF-OCT) systems for non-contact and non-invasive optical sectioning of the biological cells/tissues [1, 5]. However, the main drawback while using broad band light sources in FF-OCT is the requirement of dispersion-compensation mechanism for dispersion correction. Further, the highly absorbing biological samples exhibit inhomogeneous spectral response to different wavelengths contained in broadband light source [1, 6, 9]. These

issues overall limit the penetration depth and reduces signal to noise ratio (SNR) of FF- OCT system and further add complexity to the system. To overcome these limitations, purely monochromatic light sources like lasers can be implemented in FF-OCT system. However, high TC length of these light sources reduces the depth sectioning capability of the tomography systems [6]. Further, high TC length degrades the image quality due to the speckle noise, coherent noise and parasitic fringe formation.

On the other end, a pseudo-thermal light source, which have high TC and low SC properties, can be advantageous over all commercially available light sources: direct lasers and broadband [6, 10]. The pseudo-thermal (or quasi-thermal) light source is an extended monochromatic light source, which is generated due to the coherent light scattering from an optical rough surface. Previously, quasi-thermal light source has been synthesized by passing the laser light through the rotating diffuser [2, 4, 11] or stationary diffuser followed by a vibrating multiple multimode fiber bundle (MMFB) [12-14]. To date, their longitudinal spatial coherence (LSC) properties have been utilized in the field of profilometry, OCT and QPM [4, 6, 10, 13, 15, 16]. Significant amount of work has been reported previously for investigating coherence properties of such light sources [11, 17-20]. These types of light sources do not require any dispersion compensation mechanism for dispersion corrections while imaging biological specimens having strong dispersion or inhomogeneous spectral response [4]. In addition, implementation of this light source alleviates the problems of coherent noise, speckle noise, and parasitic fringe formation in FF-OCT systems [4, 18].

In the present letter, a synthesized pseudo thermal light source having high TC and low SC properties is reported. The longitudinal coherence (LC) properties of spatially extended monochromatic light sources synthesized from two different monochromatic laser sources: He-Ne (@ 632 nm) and DPSS (@ 532 nm), is systematically studied. The LC length of such pseudo thermal light sources is measured as a function of source size by employing Linnik based FF-OCT system and found to be minimum for large source size. Moreover, it is also observed that LC length of pseudo thermal light source does not depend on TC length of the parent laser for source size greater than 3.3 mm. At this source size, numerical aperture (NA) of the objective lens (10X and 0.30 NA in our case) becomes dominant over the TC length of the primary laser and leads to high axial resolution of ~ 15 micron. The axial resolution of the FF-OCT system is further improved by employing high NA (1.2) objective lens and found to be equal to 650 nm. The spatially extended monochromatic light source encompasses the advantages of both pure monochromatic laser and the broadband light source. This opens an opportunity to use such light sources for OCT applications with various advantages.

In the coherence theory of optical fields, the generalized van Cittert–Zernike theorem relates LSC function to the spatial structure (i.e., angular frequency

spectrum) of the quasi monochromatic extended light source [6]. Analogous to the Wiener–Khintchine theorem [7], the generalized van-Cittert–Zernike theorem [6, 7] states that LSC function 'Γ(δz, Δt=0)' and source angular frequency spectrum form Fourier transform pairs. The LSC function is defined as follows:

$$\Gamma(\delta z, \Delta t = 0) = \int_{-\infty}^{\infty} S(k_z) \exp(ik_z \delta z)\, dk_z, \qquad (1)$$

where Γ(δz, Δt=0) is the LSC function and $S(k_z)$ is the angular frequency spectrum of the light source, δz $(= z_1 - z_2)$ is the separation between spatial points $Q_1(z_1)$ and $Q_2(z_2)$ situated in two different observation planes along the propagation direction of field, and k_z is the longitudinal spatial frequency [8].

The modified expression of the LC length (Lc) which depends on the angular frequency spectrum, temporal frequency spectrum and size of the light source, can be expressed as [6, 8]:

$$L_c = \left[\frac{2\sigma^2 \sin^2\left(\theta_z/2\right)}{\lambda} + \frac{\Delta\lambda}{\lambda^2}\sigma^2 \cos^2\left(\theta_z/2\right) \right]^{-1} \qquad (2)$$

where, θz is half of the maximum angular spectrum width, λ is the central wavelength, Δλ is related to the temporal spectrum width of the source and σ is a fill factor of the objective lens which depends on the source size i.e. size of the aperture A. The fill factor 'σ' is defined as follows [6]:

$$\sigma = \frac{\varphi_2}{\varphi_1} \qquad (3)$$

where, φ_1 is full back aperture of microscope objective (MO_3) and φ_2 the beam spot size at the back aperture of MO_3 which depends on the source size A and lenses L_1, L_2 (Fig. 1d).

The experimental scheme of FF-OCT system is illustrated in Fig. 1a, which is based on the principle of non-common-path Linnik based interference microscopy. A sample mirror is positioned under FF-OCT system for the measurement of LSC length of pseudo thermal light source as a function of aperture size. The laser light beams coming from He-Ne (l_c= 15 cm) and DPSS laser (l_c= 6 mm) are split into two beams using beam splitter BS_1.

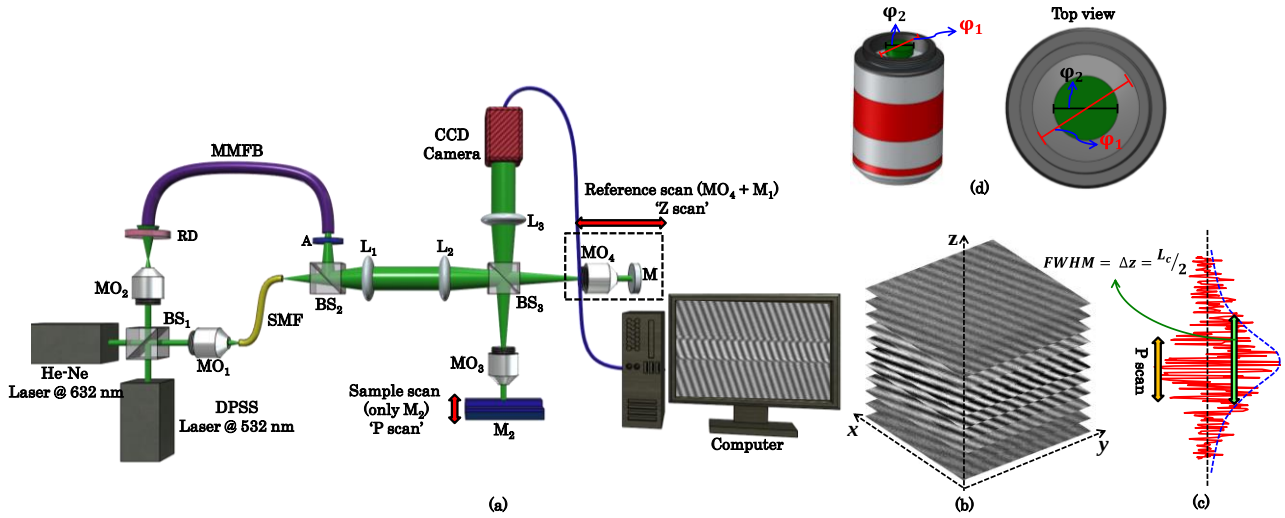

Fig. 1. (a) Schematic diagram of the spatial coherence gated FF-OCT system. $MO_{1\text{-}4}$: Microscope objectives; $BS_{1\text{-}3}$: Beam splitters; $L_{1\text{-}3}$: Lenses; RD: Rotating diffuser; MMFB: Multiple multi-mode fiber bundle; SMF: Single mode fiber; A: Variable aperture; M: Mirror and CCD: Charge coupled device. P-scan: vertical scan of mirror M_2 for LSC length measurement and Z-scan: horizontal scan of microscope objective MO_4 and mirror M_1 assembly (enclosed in black dotted box) for the measurement of temporal coherence length of light source. (b) Stack of the recorded interferograms obtained by translating mirror M_2 (Fig. 1a) along the vertical direction. (c) Variation of intensity at a particular pixel of interferogram's stack along z- direction for the quantification of FWHM of the visibility curve depicted in blue dotted curve, which provides axial resolution 'Δz' of the system, (d) microscope objective aperture showing the illuminated part with green color.

One of the beams goes towards microscope objective MO_1 which couples both light beams into a single mode fiber (SMF) to generate spatially filtered temporally high and spatially high coherent light beam. The other one goes towards microscope objective MO_2 which illuminates the rotating diffuser (RD) with a diverging beam (spot size at diffuser plane ~ 4 mm). The RD generates temporally varying speckle field and eventually reduces the speckle contrast significantly [21]. The scattered photons are directly coupled into a multiple multi-mode fiber bundle (MMFB) placed at ~ 1 mm distance from the diffuser plane to maximize the number of coupled photons into MMFB. The diameter of MMFB is 5 mm and contains hundreds of fibers (core diameter of each fiber ~ 0.1 mm). The RD followed by MMFB generates uniform illumination, i.e., speckle free field, at the output port of MMFB, which acts as an extended purely monochromatic light source namely pseudo thermal light source. Thus, generates a temporally high and spatially low coherent light source having short LSC length which depends on the spatial extent of the light source.

The output port of MMFB is attached with the input port of interference microscopy system (Fig. 1a). A variable aperture (A) is placed between output port of MMFB and input port of microscope, which controls the SC (lateral and longitudinal both) properties, i.e., LSC length, of the pseudo thermal light source. The light beams coming from SMF and MMBF are recombined using BS_2, which directs ~ 50% intensity of both the light

beams towards Linnik interferometric system. The combination of lenses L_1 and L_2 relay the source image (fibers of MMFB) at the back focal plane of the microscope objective MO_3 to achieve uniform illumination at the sample plane. The beam splitter BS_3 splits the input beam into two; one is directed towards the sample (M_2) and the other one towards reference mirror (M_1). Both the light beams reflected back from M_2 and M_1 recombine and forms interference pattern at the same beam splitter plane, which is projected at the camera plane with the help of L_3. The angle of reference mirror M_1 controls the angle between the object and the reference beam, i.e., the fringe width of the interferogram. The reference mirror M_1 is kept at a particular angle for which high fringe density without aliasing effect is observed at the change coupled device (CCD) plane. The CCD camera [Lumenera Infinity 2, 1392 × 1024 pixels, pixel size: 4.65×4.65 μm^2] is utilized for all interferometric recordings @ 30 FPS. The power at the sample is measured to be equal to 200 μW. The computational processing time was ~ 2 s.

For the measurement of LSC length or axial resolution (i.e., LSC/2), a flat mirror M_2 (Fig. 1a) as a test sample is placed under the interference microscope and scanned vertically in a constant step (1 and 0.2 μm) from – z to + z (P scan) to sequentially acquire a series of interferograms. The series of interferograms are then stacked along the z direction as presented in Fig. 1b for the measurement of LSC function of the light source. The variation of intensity at a particular pixel of interferogram's stack (Fig. 1b) is plotted as a function of z as depicted in Fig. 1c. The blue dotted curve illustrated in Fig. 1c exhibits the LSC function of pseudo thermal light source. It is observed that the fringe visibility of interferograms reduces as M_2 go away from the focal position of microscope objective MO_3. The FWHM of the LSC function thus obtained provides information about the axial resolution 'Δz' and subsequently LSC length (=$2\Delta z$) of synthesized light source.

A systematic study is done to understand the influence of source size on the LC length of pseudo thermal light source. The size of the source is varied in a step of 0.5 mm from 0.8 mm to 4.3 mm with the help of variable aperture 'A'. Two microscope objective lenses MO_3 and MO_4 having NA 0.3 (10×) are utilized in Linnik interference microscopy system. The LC length of extended monochromatic light source synthesized from two high coherent lasers: DPSS laser (l_c~ 6 mm) and He-Ne laser (l_c ~ 15 cm) is measured as a function of source and compared. Figures 2a – 2h present the normalized LC functions of pseudo thermal light source for different source sizes (D) at two different wavelengths. The LC functions illustrated in green and red color profiles (Figs. 2a – 2h) correspond to 532 nm and 632 nm wavelengths, respectively. The x-axis limit of the line plots is kept different to clearly visualize the difference in FWHM of the visibility curves for 532 nm and 632 nm. A slight asymmetry in the measured LC functions could be due to slight misalignment in the beam path. The FWHM of each LC functions corresponding to 532 nm and 632 nm wavelengths are then calculated to obtain LC length and subsequently axial resolution of the system.

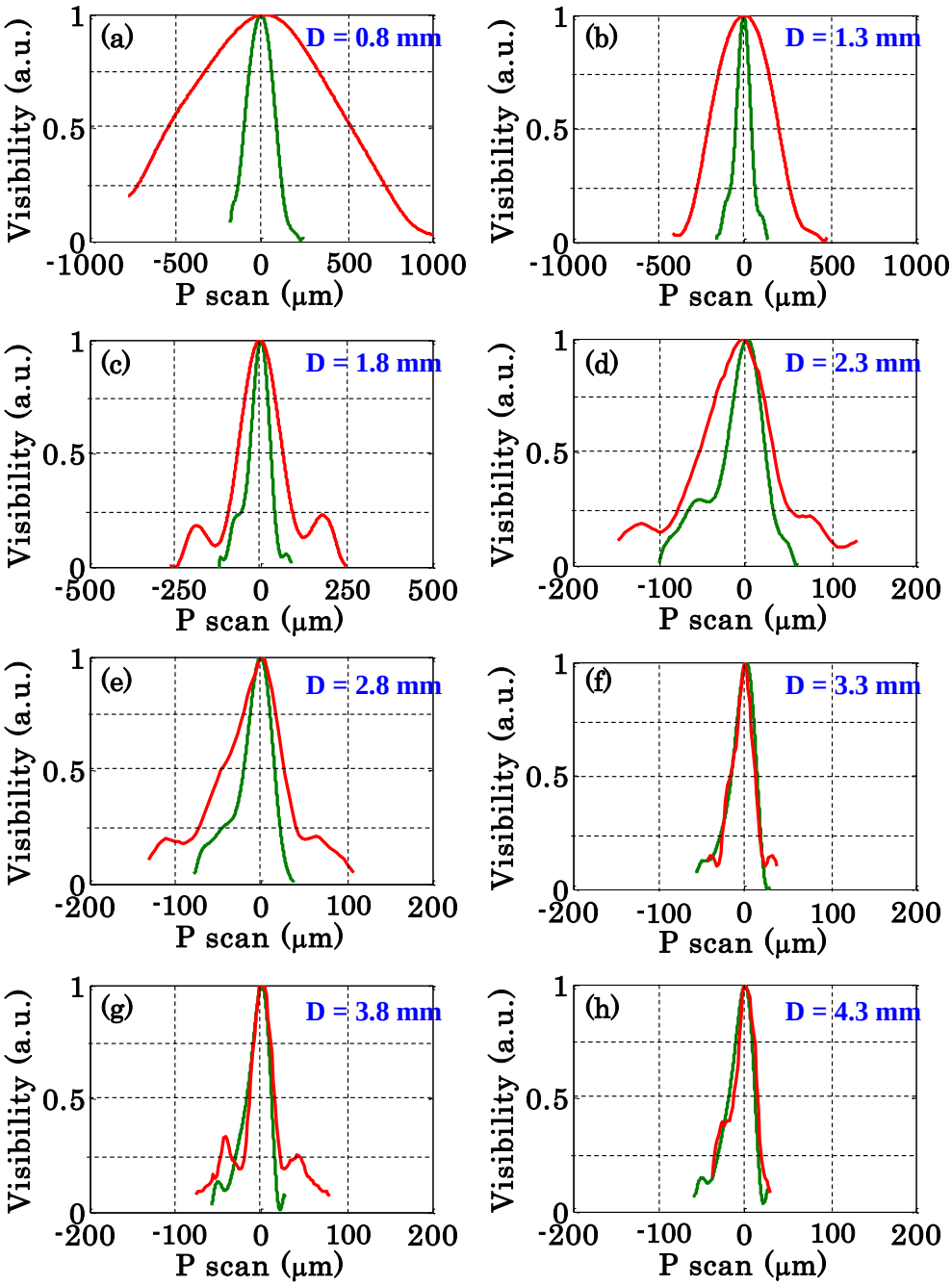

Fig. 2. The LC functions of extended monochromatic light source synthesized from two high coherent lasers: DPSS laser (l_c ~ 6 mm) and He-Ne laser (l_c ~ 15 cm) as a function of source sizes: (a – h) 0.8 – 4.3 mm in a step of 0.5 mm. Green and red color curves represent the LC functions corresponding to 0.3 NA objective lens at 532 nm and 632 nm wavelengths, respectively. D is the source size in mm.

Figures 3a and 3b represent the variation of LC length as a function of source size of pseudo thermal light source synthesized from DPPS(@ 532 nm) and He-Ne(@ 632 nm) laser. The y-axis limit of the line plots is kept different to clearly see the trend of LC length variation with source size for 532 nm and 632 nm. It can be clearly seen that LC length

decreases as the size of aperture increases. The maximum LC length was obtained for source size of 0.8 mm for both the wavelengths. However, LC length measured at 632 nm wavelength is found to be large compared to 532 nm wavelength. When the large source size ≥ 3.3 mm is used, the LC length becomes independent on the TC length of the parent laser source and approached to a constant value of about ~ 30 µm. Thus LC length of the pseudo-thermal source is reduced significantly down to 30 µm from ~ 1 mm. The axial resolution would be equal to half of the LC length, i.e., ~ 15 µm. This can be explained from Eq. 2. For a small source size, LC length is decided by both temporal and spatial coherence terms of the source. However, for large aperture size (i.e., wide angular spectrum light source), TC term can be neglected compared to LSC term, thus, LC is purely determined by only LSC term.

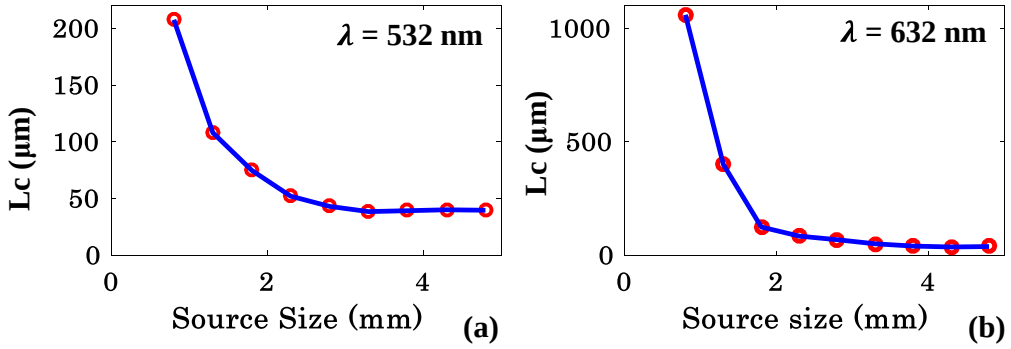

Fig. 3. The LC length of extended monochromatic light source synthesized from two high coherent lasers: (a) DPSS laser @ 532 nm and (b) He-Ne laser @ 632 nm as a function of source size.

The LSC length, i.e., axial resolution, of the system can be further improved with the employment of high NA objective lens as use of high NA widen the angular spectrum light source [6]. To exhibit the improvement in axial resolution, experiments are conducted with water immersion objective lens (1.2 NA) at 632 nm wavelength. The mirror M_2 is scanned vertically in a step of 0.2 µm to record a series of interferograms for the measurement of LC length. Figure 4 presents the visibility curve of the pseudo-thermal light source for 0.8 mm and 3.3 mm source sizes. The axial resolution (half of the LC length), i.e., FWHM of the visibility curve, is measured to be equal to 1.7 µm and 650 nm, respectively. The short LC length (~ 1.3 µm) thus achieved may find potential application in high resolution optical sectioning of multilayered biological specimens irrespective of the high TC length of parent laser source. The transverse resolution is measured to be equal to 1.2 µm for 0.3 NA objective lens.

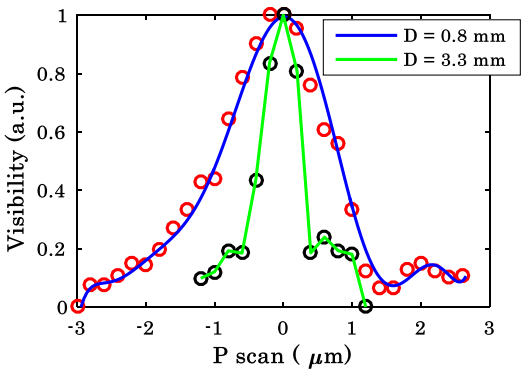

Fig. 4. The axial resolution of pseudo-thermal light source corresponding to water immersion objective lens (1.2 NA) at 632 nm wavelength and source sizes of 0.8 mm and 3.3 mm.

In conclusion, high resolution optical sectioning of the samples is possible with the pseudo thermal, i.e., purely monochromatic (i.e., high TC length) extended light source which is otherwise not possible with the direct laser. This is contrary to the principle of conventional FF-OCT system, which performs high resolution sectioning by utilizing low TC property of broadband light source. The influence of source size on the LC coherence properties of pseudo thermal light source is systematically studied. The axial resolution is measured to be equal to ~ 15 µm for pseudo thermal source size of 3.3 mm and 0.3 NA objective lens. The axial resolution of the system is found to be independent on the TC lengths of the primary laser: DPSS (l_c ~ 6 mm) and He-Ne (l_c ~ 15 cm) lasers at 3.3 mm source size. The axial resolution of the system is further improved by employing 1.2 NA objective lens and measured to be equal to 650 nm at 632 nm wavelength. Thus, use of a sufficiently wide angular spectrum, i.e., low LSC length, synthesized light source enables high resolution sectioning of the specimen irrespective of the TC length of the direct laser. The use of such light sources are advantageous as it does not require any dispersion compensation and chromatic aberration corrected optics, which are mandatory in case of broadband light sources [4]. In addition, any narrowband light source of suitable wavelength falling in the biological window can be employed for speckle free high resolution optical sectioning. Future work will focus on performing high-axial resolution FF-OCT applications on biological samples using pseudo-thermal sources.

Funding. The authors are thankful to Department of Atomic Energy (DAE) for financial grant no. 34/14/07/BRNS. Authors also would like to acknowledge University Grant Commission (UGC) India and Norwegian Centre for International Cooperation in Education, SIU-Norway (Project number INCP- 2014/10024) for joint funding.

References

1. W. Drexler and J. G. Fujimoto, *Optical coherence tomography: technology and applications* (Springer Science & Business Media, 2008).

2. F. Dubois, M.-L. N. Requena, C. Minetti, O. Monnom, and E. Istasse, "Partial spatial coherence effects in digital holographic microscopy with a laser source," Appl. Opt. **43**, 1131-1139 (2004).

3. G. Popescu, *Quantitative phase imaging of cells and tissues* (McGraw Hill Professional, 2011).

4. J. Rosen and M. Takeda, "Longitudinal spatial coherence applied for surface profilometry," Appl. Opt. **39**, 4107-4111 (2000).

5. H. M. Subhash, "Full-field and single-shot full-field optical coherence tomography: A novel technique for biomedical imaging applications," Advances in Optical Technologies **2012**(2012).

6. I. Abdulhalim, "Spatial and temporal coherence effects in interference microscopy and full-field optical coherence tomography," Ann. Phys. **524**, 787-804 (2012).

7. L. Mandel and E. Wolf, *Optical coherence and quantum optics* (Cambridge university press, 1995).

8. V. Ryabukho, D. Lyakin, A. Grebenyuk, and S. Klykov, "Wiener–Khintchin theorem for spatial coherence of optical wave field," J. Opt. **15**, 025405 (2013).

9. L. Vabre, A. Dubois, and A. C. Boccara, "Thermal-light full-field optical coherence tomography," Opt. Lett. **27**, 530-532 (2002).

10. D. S. Mehta, V. Srivastava, S. Nandy, A. Ahmad, and V. Dubey, "Full-Field Optical Coherence Tomography and Microscopy Using Spatially Incoherent Monochromatic Light," in *Handbook of Full-Field Optical Coherence Microscopy* (Pan Stanford, 2016), pp. 379-414.

11. M. Gokhler and J. Rosen, "General configuration for using the longitudinal spatial coherence effect," Opt. Commun. **252**, 22-28 (2005).

12. A. Ahmad, V. Dubey, V. Singh, A. Butola, T. Joshi, and D. S. Mehta, "Reduction of spatial phase noise in the laser based digital holographic microscopy for the quantitative phase measurement of biological cells," in *European Conference on Biomedical Optics*, (Optical Society of America, 2017), 104140H.

13. A. Ahmad, V. Srivastava, V. Dubey, and D. Mehta, "Ultra-short longitudinal spatial coherence length of laser light with the combined effect of spatial, angular, and temporal diversity," Appl. Phys. Lett. **106**, 093701 (2015).

14. A. Ahmad, V. Dubey, G. Singh, V. Singh, and D. S. Mehta, "Quantitative phase imaging of biological cells using spatially low and temporally high coherent light source," Opt. Lett. **41**, 1554-1557 (2016).

15. P. Pavliček, M. Halouzka, Z. Duan, and M. Takeda, "Spatial coherence profilometry on tilted surfaces," Appl. Opt. **48**, H40-H47 (2009).

16. A. Safrani and I. Abdulhalim, "Ultrahigh-resolution full-field optical coherence tomography using spatial coherence gating and quasi-monochromatic illumination," Opt. Lett. **37**, 458-460 (2012).

17. V. Ryabukho, D. Lyakin, and M. Lobachev, "Longitudinal pure spatial coherence of a light field with wide frequency and angular spectra," Opt. Lett. **30**, 224-226 (2005).

18. I. Abdulhalim, "Competence between spatial and temporal coherence in full field optical coherence tomography and interference microscopy," J. Opt. A: Pure Appl. Opt. **8**, 952 (2006).

19. V. Ryabukho, A. Kal'yanov, D. Lyakin, and V. Lychagov, "Influence of the frequency spectrum width on the transverse coherence of optical field," Opt. Spectrosc. **108**, 979-984 (2010).

20. V. Ryabukho and D. Lyakin, "The effects of longitudinal spatial coherence of light in interference experiments," Opt. Spectrosc. **98**, 273-283 (2005).

21. J. W. Goodman, *Speckle phenomena in optics: theory and applications* (Roberts and Company Publishers, 2007).